PAPER

A nanofluidic device for single molecule studies with *in situ* control of environmental solution conditions

Ce Zhang,[a] Kai Jiang,[a] Fan Liu,[a] Patrick S. Doyle,[bc] Jeroen A. van Kan[a] and Johan R. C. van der Maarel*[ac]

We report an approach to study the *in situ* conformational response of single biomolecules such as DNA to a change in environmental solution conditions. These conditions are, for example, the composition of the buffer or the presence of protein. For this purpose, we designed and fabricated a nanofluidic device featuring two arrays of parallel nanochannels in a perpendicular configuration. The cross-sections of the channels are rectangular with a diameter down to 175 nm. These lab-on-a-chip devices were made of polydimethylsiloxane (PDMS) cast on a high quality master stamp, obtained by proton beam writing and UV lithography. Biomolecules can be inserted into the device through the array of channels in one direction, whereas the buffer can be exchanged through the intersecting array of channels in the other direction. A buffer exchange time inside the grid of nanochannels of less than one second was measured by monitoring the conductivity of salt solutions. The exchange time of a protein was typically a few seconds, as determined by imaging the influx of fluorescence labelled protamine. We demonstrate the functionality of the device by investigating the compaction of DNA by protamine and the unpacking of pre-compacted DNA through an increase in the concentration of salt.

1 Introduction

Single molecule techniques are now routinely employed to investigate the properties of biomacromolecules, including double stranded DNA. In order to observe a conformational response to, for example, the binding of a protein, the molecule needs to be trapped so that it is not moved away by the exchanging protein carrying buffer. Trapping often requires chemical modification of the molecule under investigation. A well-known example is the attachment of a colloidal bead to the end of a DNA molecule in an optical or magnetic tweezers setup.[1–4] Anchoring or tethering the molecule can however be problematic in certain applications. These applications include the investigation of closed circular DNA or sequential measurements in lab-on-a-chip devices. Here, we present a nanofluidic device, which allows the study of single molecules in their native state with the possibility of *in situ* control of the environmental solution conditions.

Advances in nanofabrication have made it possible to fabricate quasi one-dimensional channel devices with cross-sectional diameters in the range of tens to hundreds of nanometers. These channels serve as a platform for studying single DNA molecules, amongst others.[5–14] Nanochannels are also important for single-molecule technologies used to study large-scale genomic organisation, including restriction enzyme cutting, nick labelling and denaturation mapping.[15–17] Advantages of the nanochannel platform are that the DNA molecules are in an equilibrium conformation, high through-put can be achieved by using arrays of parallel channels and integration with lab-on-a-chip devices.[18] The molecules are usually visualised with fluorescence microscopy.

Our device features two arrays of parallel nanochannels in a perpendicular configuration.[19] The channels are rectangular with cross-sectional dimensions of 200×150 nm^2 and 200×150 nm^2 in the two perpendicular directions, respectively. The chips are made of polydimethylsiloxane (PDMS) cast on a high quality master stamp, obtained by proton beam writing and UV lithography.[22–24] The advantage of this technology is that about a hundred replicas can be made with a single stamp, so that a fresh chip can be used for every experiment. We show that DNA can be inserted into the device through the array of wider nanochannels in one direction. Inside these channels, the DNA molecules are stretched and prevented from exiting due to the entropic barrier provided by the narrower channels.[20,21] The buffer can subsequently be exchanged through the intersecting array of nanochannels in the other direction. The exchange time of the buffer is determined by monitoring the current through the channels following an increase in concentration of salt. We also measured the time required for the exchange of protein by imaging fluorescence labelled protamine. Finally, we demonstrated the functionality

[a]*Department of Physics, National University of Singapore, Singapore 117542*
[b]*Department of Chemical Engineering, Massachusetts Institute of Technology, Cambridge, Massachusetts 02139, United States of America*
[c]*BioSystems and Micromechanics, Singapore-MIT Alliance for Research and Technology, Singapore. E-mail: johanmaarel@gmail.com*

of the device by investigating the compaction of DNA by protamine and the unpacking of pre-compacted DNA through an increase in concentration of salt.

2 Materials and methods

2.1 Chip fabrication

The nanofluidic devices were fabricated in PDMS using patterned master stamps to replicate.[22] The grid of nanochannels was made in HSQ resist (Dow Corning, Midland, MI) using a lithography process with proton beam writing.[23,24] The two intersecting arrays of nanochannels are connected to a superposing set of microchannels made in SU-8 resin with UV lithography. To promote the release of the PDMS replica, the stamp was coated with a layer of teflon with a thickness of 5 nm and baked at 393 K for 12 h.[25] The perpendicular nanochannels have widths of 150 ± 10 nm and 250 ± 10 nm respectively, measured using scanning electron microscopy. The height of the positive channel structure is 200 ± 5 nm, as determined by atomic force microscopy (Dimension 3000, Veeco, Woodbury, NY). The microchannels have a length, width and height of 1 mm, 30 μm and 5 μm respectively. The stamps were replicated in PDMS followed by curing with a curing agent (Sylgard, Dow Corning) at 338 K for 24 h. Two pairs of loading reservoirs (1.0 mm diameter) were punched in the PDMS replica. The replica was sealed with a glass coverslip, after which both substrates were plasma oxidised (Harrick, Ossining, NY).

2.2 Sample preparation

T4–DNA was purchased from Nippon Gene, Tokyo and used without further purification. YOYO–1 was purchased from Invitrogen, Carlsbad, CA. T4–DNA was stained with YOYO–1 with an intercalation ratio of 100 base-pairs per dye molecule. Samples were prepared by dialysing solutions of T4–DNA against 10 mM Tris/HCl ($1 \times$ T) buffer in micro-dialysers. The Tris was adjusted with HCl to pH 8.5, *i.e.* 2.9 mM TrisCl and 7.1 mM Tris. The ionic strength of the buffer was calculated using the Davies equation to estimate the activity coefficients of the ions and the dissociation constant pK = 8.08 for Tris. Protamine chloride from salmon was purchased from Sigma-Aldrich and dissolved in the Tris/HCl buffer. For the pre-equilibrated samples, solutions of protamine and DNA were mixed in equal volumes and incubated for 24 h at 277 K. The final DNA concentration was 3 mg L^{-1}. The buffer used for unpacking of DNA inside the channels was of the same composition, but with 100 mM of added NaCl. No anti-photobleaching agent was used, since it might interfere with protein-DNA binding. Fluorescein 5-isothiocyanate (FITC) was purchased from Sigma-Aldrich. Protamine was labelled with FITC following the standard protocol.[26] For the determination of the time required for protein exchange, a solution of 1 μM of protamine in $1 \times$ T buffer was prepared.

2.3 Conductivity measurements

All loading reservoirs and channels of the chip were initially filled with $1 \times$ T buffer. At a pre-set time, about 50 μL of a solution of 30 mM or 2 M NaCl was pipetted into one of the reservoirs using a microinjector with a minimal pressure of 0.5 kPa (Narishige, Tokyo). Note that the pipette of the micro-injector was not sealed to the reservoir. The salt ions were subsequently transported through the microchannel and the intersecting array of 200×150 nm^2 channels into the 200×250 nm^2 channels by combination of the minimal hydrostatic pressure resulting from the filling of the reservoir and diffusion. The exchange of buffer was monitored by measuring the current through the array of 200×250 nm^2 channels with a sourcemeter (Keithley 237, Cleveland, Ohio) and an applied voltage of 200 V across the corresponding loading reservoirs.

2.4 Protein exchange

Prior to protein exchange, all reservoirs and channels were filled with $1 \times$ T buffer. Fluorescence stained protamine was pipetted into one of the reservoirs and exchanged through the microchannel and intersecting array of 200×150 nm^2 channels into the 200×250 nm^2 channels as described above. The stained protein was visualised using a Nikon Eclipse Ti inverted fluorescence microscope equipped with a 200 W metal halide lamp, a filter set and a $100 \times$ oil immersion objective lens. A UV light shutter controlled the exposure time. A series of images were collected with an electron multiplying charge coupled device (EMCCD) camera (Andor iXon X3).

2.5 DNA compaction and unpacking

The stained DNA molecules dispersed in the relevant buffer were loaded into the two reservoirs connected to the array of 200×250 nm^2 channels. To maintain a balanced pressure, $1 \times$ T buffer (without DNA) was loaded into the other two reservoirs connected to the perpendicular, intersecting array of 200×150 nm^2 channels. The DNA molecules were subsequently driven into the channels by electrophoresis. For this purpose, two platinum electrodes were immersed in the relevant reservoirs and connected to an electrophoresis power supply with a relatively low voltage in the range 0.1–10 V (Keithley, Cleveland, Ohio). Once the DNA molecules were localised inside the nanochannels, the electric field was switched off and the molecules were allowed to relax to their equilibrium state for at least 60 s. At pre-set times, protamine was pipetted into one of the reservoirs and exchanged through the microchannel and intersecting array of 200×150 nm^2 into the 200×250 nm^2 channels as described above. During and following exposure to protamine, the DNA molecules were visualised using the above-mentioned imaging system and their extensions were measured with ImageJ software (http://rsb.info.nih.gov/ij/).
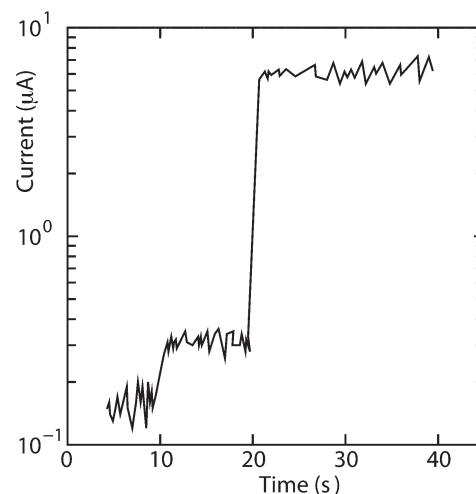
3 Results and discussion

The layout of the device is illustrated in Fig. 1. A centrally located grid of rectangular nanochannels was connected to two pairs of loading reservoirs with a set of microchannels. The grid features two arrays of parallel nanochannels in a perpendicular configuration. Both arrays have the same depth of 200 nm. In one direction, the width of the individual
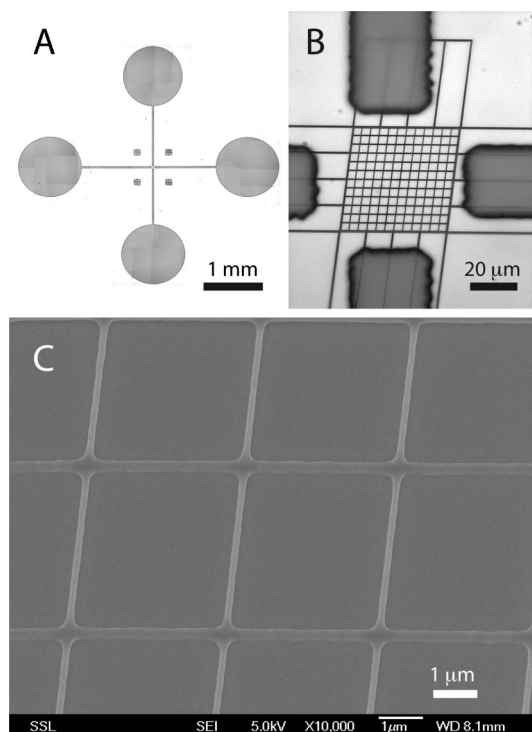
Fig. 1 (A) Bright field optical image of the bonded lab-on-a-chip device. The loading reservoirs are connected to the central grid of nanochannels by microchannels in SU-8 resin. (B) Optical image of the master stamp featuring the nanochannel grid with connecting microchannels. (C) Scanning electron micrographs of the central HSQ master showing a positive standing crossed-channel structure with widths of 250 and 150 nm and a uniform height of 200 nm. The wide and narrow channels are laid on a rectangular grid and separated by 4.0 and 3.75 μm, respectively.

Fig. 2 Current through the array of 200×250 nm^2 channels with an applied voltage of 200 V across the loading reservoirs. Initially, the channels contain $1 \times$ T buffer. At times $t = 10$ and 20 s, solutions of 30 mM and 2 M NaCl, respectively, were exchanged through the perpendicular, intersecting array of 200×150 nm^2 channels into the 200×250 nm^2 channels.

channels is 250 nm (wide channels). In the other direction, the width is 150 nm (narrow channels). As shown below, DNA can easily be brought into the array of wide channels with the help of an electric field. The buffer containing (for example) protein can then be exchanged through the array of narrow into the wide channels. In order to gauge the concomitant response in the conformation of the confined DNA molecules, it was necessary to calculate the time required to exchange the buffer for our device.

In the first series of experiments, the channels and loading reservoirs were filled with $1 \times$ T buffer. This buffer had an ionic strength of around 3 mM. We measured the current through the array of wide channels with an applied voltage of 200 V across the corresponding set of loading reservoirs. At pre-set times, solutions with increasing concentrations of NaCl were subsequently pipetted into one of the reservoirs connected to the array of narrow channels. The current through the wide channels was monitored and is shown in Fig. 2. Once the salt penetrated the wide channels, the current jumped to a higher value pertaining to a higher concentration of salt. The jump in current occurred within a lag-time of about 2 s after the salt solution was transferred by pipette into the reservoir, whereas the duration of the jump itself was less

than 1 s. Accordingly, the exchange rate for buffers containing a higher concentration of low molecular weight salt is relatively fast. The short lag-time indicates that transport through the feeding microchannel is facilitated by a combination of diffusion and convection through hydrostatic pressure gradients resulting from filling of the loading reservoir. Once the ions reach the entrance of the nanochannels, diffusion is expected to be the main mechanism of transport. For one-dimensional diffusion, the front of the concentration profile is displaced by a distance $\Delta x = 2(Dt)^{1/2}$ over time t. With a diffusion coefficient $D = 1.5 \times 10^{-9}$ m^{2}s^{-1} of NaCl and a length of the nanochannels $\Delta x = 45$ μm, the time taken to fill the grid of nanochannels is estimated to be 0.3 s.[27] This filling time agrees with the short duration of the jump. Since transport through the nanochannels is largely determined by diffusion, the rate of exchange is expected to depend on molecular weight and can be different for each protein.

In a second series of experiments, a buffer containing 1 μM FITC-labelled protamine ($M_w \approx 5.1$ kDa) was transferred by pipette into one of the loading reservoirs connected to the array of narrow nanochannels. Using fluorescence microscopy to monitor the protein being transported through the microchannel, this reached the entrance of the nanochannels in about 30 s. This time is significantly shorter than might be expected based on diffusion (minutes), so convection resulting from the pipetting of the protein solution into the reservoir and concomitant hydrostatic pressure gradients also plays a role. Subsequently, the protein was transported through the narrow into the wide channels. Fig. 3 shows the time evolution of the integrated fluorescence intensity across the array of narrow channels. The buffer is progressively and uniformly replaced within about 3 s from the moment the protein enters the array of nanochannels. For one-dimensional diffusion, the
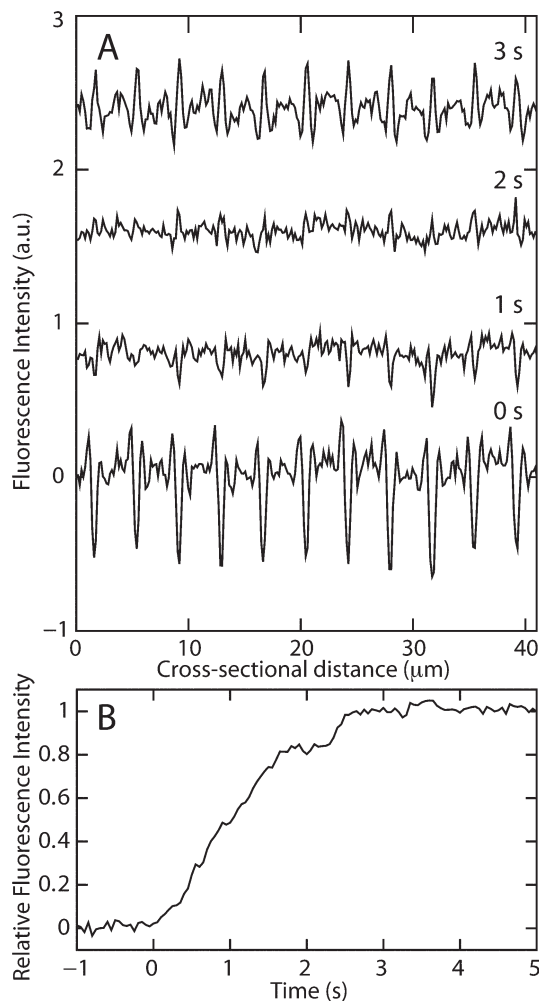
Fig. 3 (A) Fluorescence intensity profile across the array of 200 × 150 nm² channels imaged at the indicated times during the exchange of FITC-labelled protamine. The channels are separated by 3.75 μm. (B) Integrated fluorescence intensity as a function of elapsed time. Time = 0 is defined as the moment when the protein enters the nanochannels and the fluorescence intensity starts to increase.

concentration profile of protamine with diffusion coefficient $D = (1.2 \pm 0.1) \times 10^{-10}$ m²s⁻¹ covers the 45 μm length of the nanochannels in 4.2 s.[28] The experimental exchange time of the protein inside the grid of nanochannels therefore agrees with a diffusion driven process. Eventually, the protein exits through the nanochannels into the microchannels connected to the other reservoirs. We have verified that, due to the continuous influx of protein, there is no appreciable drop in the integrated fluorescence intensity and, therefore, the protein concentration for longer times. Furthermore, we did not observe adhesion of protamine to the surface of PDMS. There is accordingly no need for passivation of the channel walls, as might be required for devices made of fused silica.[29]

In the third and fourth series of experiments, we demonstrated the functionality of the device with an application study of DNA compaction and unpacking of pre-compacted DNA, respectively. We used protamine as the compaction

agent. Protamines are arginine-rich proteins that replace histones during spermatogenesis. As a result of this replacement, DNA is compacted into a condensed structure.[30] The extent of the compaction depends on the concentration of protamine and the ionic strength of the supporting buffer medium.[1,31] Inside the regular, rectangular nanochannels with a cross section of 300 × 200 nm², we verified that T4–DNA can be compacted with 0.4 μM of protamine in 1 × T buffer. With the addition of 10 mM NaCl to the 1 × T buffer, the threshold for compaction decreased about tenfold to a protamine concentration of 0.03 μM. In the case of 1 × T buffer with 100 mM of added NaCl, no compaction of the DNA was observed up to and including a protamine concentration of 5 μM. Accordingly, DNA compacted by protamine can subsequently be unpacked with a buffer of high ionic strength. These results obtained for regular nanochannels mark the conditions in terms of the range of protamine and salt concentrations for our experiments with the cross-channel device.

For the third series of experiments, T4–DNA molecules immersed in 1 × T buffer were electrophoretically driven into the array of wide nanochannels. Pressure gradients were minimised by filling the other two loading reservoirs with 1 × T buffer. Once the electric field was removed, the molecules equilibrated and remained stationary inside the array of wide channels. Since the ionic strength of the 1 × T buffer was sufficiently low (about 3 mM), the initial stretching of the molecules along the direction of the channel is around 10 μm (*i.e.*, a relative extension of 0.17 times the YOYO–1 corrected contour length of 57 μm). Protamine was pipetted into one of the reservoirs and exchanged through the array of narrow channels into the wide channels. Throughout the exchange of buffer, the DNA molecules were imaged using fluorescence microscopy. This showed that they remain trapped, due to the small cross-sectional area of the intersecting, narrow channels and a channel spacing less than the stretch of the DNA molecule (3.75 *vs.* 10 μm). Furthermore, we observed that the molecules remained mobile and that there was no protamine-mediated sticking of DNA to the channel walls.

A time-lapse series of fluorescence images of T4–DNA, captured after exposure to protamine, as well as the relative extension are shown in Fig. 4. It can be seen that the timescale of compaction depends on the concentration of protamine: the compaction times are 8, 4 and 3 s for 1, 3 and 5 μM protamine, respectively. These times are consistent with those reported in the literature based on the compaction of DNA tethered to optical tweezers in a flow cell.[1] It should be noted that the compaction times are somewhat longer than the above reported time required for the influx of 1 μM protamine into the nanochannels (3 s). This suggests that the binding of protamine on DNA with concomitant folding into the compacted state is the time limiting factor. Close inspection of the fluorescence images reveals that the compaction often starts at the ends of the molecule, but nucleation somewhere in the middle also occurs. This latter observation is at odds with the previously reported results for tethered DNA in a flow
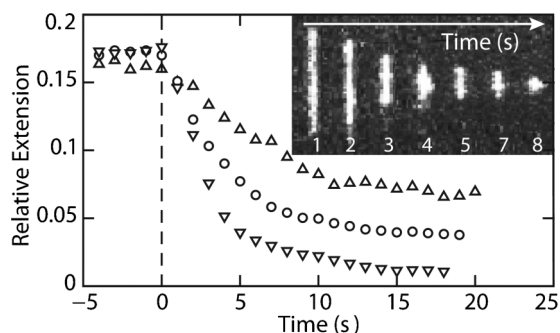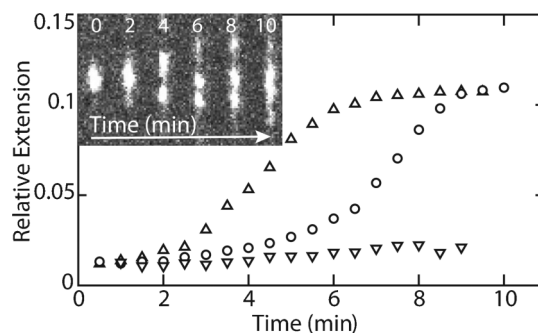
Fig. 4 Compaction of T4–DNA following exposure to a solution of 1 (△), 3 (○) and 5 (▽) μM protamine in 1 × T buffer. The DNA molecules are confined in channels with a cross-section of 200 × 250 nm². The data represent average trajectories pertaining to the compaction of five different molecules. The inset shows a time-lapse series of fluorescence images pertaining to the compaction following exposure to 5 μM protamine in 1 × T buffer. Time zero is defined as the moment when the molecules start to compact.

Fig. 5 Unpacking of T4–DNA following exposure to a solution of 1 (△), 3 (○) and 5 (▽) μM protamine in 1 × T buffer and 100 mM NaCl. Prior to unpacking, the DNA molecules were brought into the array of 200 × 250 nm² channels in compacted form. The data represent averages pertaining to the unpacking of five different DNA molecules. The inset shows a time-lapse series of fluorescence images pertaining to unpacking following exposure to 1 μM protamine in 1 × T buffer and 100 mM NaCl.

cell, where compaction was exclusively observed to start at the dangling end.[1] Note that the spacing of the channels is less than the stretch of the molecule in its elongated state. Nucleation somewhere in the middle can be explained by the fact that central parts of the molecule might be exposed to higher local concentrations of protamine in the vicinity of the intersecting feeding channels.

In addition to the compaction time, the final size of the compacted molecules inside the channels depends on the concentration of protamine. For 1, 3 and 5 μM protamine the compacted molecules have an extension along the channel of 3, 2 and 0.6 μm, respectively. These extensions show that the segment density of the compacted molecules depends on the concentration of the condensation agent. Compacted DNA usually has an ordered morphology, in which the segments are arranged in a hexagonal fashion.[32] Inside the nanochannel, the structural arrangement of the compacted molecules is probably also hexagonal. However, this could not be confirmed, because of the difficulties associated with molecular imaging of enclosed molecules.

In the fourth and final series of experiments, we showed unpacking of priorly compacted DNA by an increase in ionic strength of the supporting buffer. For this purpose, T4–DNA was pre-incubated with 1 μM protamine in the bulk phase for 24 h. The compacted molecules were imaged by atomic force microscopy and observed to be toroidal.[30] These toroids were subsequently electrophoresed into the array of wide channels and allowed to equilibrate for at least 10 min. An unpacking buffer containing 1, 3 or 5 μM protamine, 1 × T and 100 mM NaCl was exchanged through the array of narrow channels into the wide channels. The time evolution of the extension of the molecules following the exchange of buffer was monitored using fluorescence microscopy and is illustrated in Fig. 5.

The initial extension of the DNA molecules brought into the channels in compacted form is around 1 μm. It is worth noting that the latter extension is significantly less than the equilibrated extension obtained for compaction *inside* the

channels with the same concentration of protamine (3 μm for 1 μM of protamine, see Fig. 4). This difference in extension shows that the segment density of the compacted molecules depends on confinement during the collapse into the globular state and/or time of incubation. It is seen that the compacted DNA molecules gradually unfold and take a progressively more extended conformation. Compacted sub-structures typically coexistent with unfolded structures, like a beads on a string structure. Furthermore, hints of tails are observed throughout the unpacking process, which indicates the initial unpacking of DNA segments at both ends of the molecule.

The unpacking time depends on the concentration of protamine. For 1 and 3 μM protamine, the unpacking times are 8 and 10 min, respectively. In the case of 5 μM protamine, the molecules did not unpack within the time span of our experiment (40 min). Overall, unpacking occurs on a timescale of minutes, which is two orders of magnitude slower than the above described compaction on a timescale of seconds. For tethered DNA in a flow cell, an unpacking time of a few seconds has been reported before.[1] The difference between the present and previous results for the unpacking time might be related to the fact that in our experiments the molecules are unpacked after incubation with protamine for 24 h. In the previous experiments the same molecule was unpacked *immediately* after compaction with protamine inside the flow cell. The prolonged time of incubation results in a more compacted globule of higher segment density as well as a longer time required for unpacking by a buffer of high ionic strength.

4 Conclusions

We have developed a nanofluidic device for the study of the conformational response of single DNA molecules to a change in buffer composition and/or the presence of a compaction agent such as protamine. We have shown that the buffer can

be exchanged without the need to anchor or tether the molecules. The times for exchange of simple salt and solutions of protamine inside the grid of nanochannels were measured to be in the range of less than a second for salt up to about 3 s for protamine. These exchange times agree with a diffusion driven process. The time taken for the protein to reach the entrance of the nanochannels from the loading reservoir is tens of seconds, but we expect that this can be reduced by optimization of the layout of the feeding microchannel system. In principle, using a sealed inlet and the application of pressure could enhance the rate of exchange. We have however refrained from pressurised injection, because of the risk of delamination of the chip and coverslip. The functionality of the device was demonstrated by investigating the compaction of DNA by protamine and unpacking of pre-compacted DNA through an increase in concentration of salt. These results prove the suitability of the device for the investigation of the conformational, dynamic response of single biomolecules such as DNA and/or their complexes with protein to an *in situ* change in environmental solution conditions.

Acknowledgements

References

1 L. R. Brewer, M. Corzett and R. Balhorn, *Science*, 2005, **286**, 120–123.

2 D. Skoko, J. Yan, R. C. Johnson and J. F. Marko, *Phys. Rev. Lett.*, 2005, **95**, 208101.

3 B. A. Todd, V. A. Parsegian, A. Shirahata, T. J. Thomas and D. C. Rau, *Biophys. J.*, 2008, **94**, 4775–4782.

4 K. Hirano, M. Ichikawa, T. Ishido, M. Ishikawa, Y. Baba and K. Yoshikawa, *Nucleic Acids Res.*, 2012, **40**, 284–289.

5 W. Reisner, K. J. Morton, R. Riehn, Y. M. Wang, Z. Yu, M. Rosen, J. C. Sturm, S. Y. Chou, E. Frey and R. H. Austin, *Phys. Rev. Lett.*, 2005, **94**, 196101.

6 J. T. Mannion, C. H. Reccius, J. D. Cross and H. G. Craighead, *Biophys. J.*, 2006, **90**, 4538–4545.

7 W. Reisner, J. P. Beech, N. B. Larsen, H. Flyvbjerg, A. Kristensen and J. O. Tegenfeldt, *Phys. Rev. Lett.*, 2007, **99**, 058302.

8 K. Jo, D. M. Dhingra, T. Odijk, J. J. de Pablo, M. D. Graham, R. Runnheim, D. Forrest and D. C. Schwartz, *Proc. Natl. Acad. Sci. U. S. A.*, 2007, **104**, 2673–2678.

9 C. Zhang, F. Zhang, J. A. van Kan and J. R. C. van der Maarel, *J. Chem. Phys.*, 2008, **128**, 225109.

10 F. Persson, P. Utko, W. Reisner, N. B. Larsen and A. Kristensen, *Nano Lett.*, 2009, **9**, 1382–1385.

11 T. Su, S. K. Das, M. Xiao and P. K. Purohit, *PLoS One*, 2011, **6**, e16890.

12 C. Zhang, P. G. Shao, J. A. van Kan and J. R. C. van der Maarel, *Proc. Natl. Acad. Sci. U. S. A.*, 2009, **106**, 16651–16656.

13 J. J. Jones, J. R. C. van der Maarel and P. S. Doyle, *Nano Lett.*, 2011, **11**, 5047–5053.

14 C. Zhang, Z. Gong, D. Guttula, P. P. Malar, J. A. van Kan, P. S. Doyle and J. R. C. van der Maarel, *J. Phys. Chem. B*, 2012, **116**, 3031–3036.

15 R. Riehn, M. Lu, Y. M. Wang, S. F. Lim, E. C. Cox and R. H. Austin, *Proc. Natl. Acad. Sci. U. S. A.*, 2005, **102**, 10012–10016.

16 S. K. Das, M. D. Austin, M. C. Akana, P. Deshpande, H. Cao and M. Xiao, *Nucleic Acids Res.*, 2010, **38**, e177.

17 W. Reisner, N. B. Larsen, A. Silahtaroglu, A. Kristensen, N. Tommerup, J. O. Tegenfeldt and H. Flyvbjerg, *Proc. Natl. Acad. Sci. U. S. A.*, 2010, **107**, 13294–13299.

18 W. Reisner, J. N. Pedersen and R. H. Austin, *Rep. Prog. Phys.*, 2012, **75**, 106601.

19 R. Riehn, R. H. Austin and J. C. Sturm, *Nano Lett.*, 2006, **6**, 1973–1976.

20 J. O. Tegenfeldt, C. Prinz, H. Cao, S. Chou, W. W. Reisner, R. Riehn, Y. M. Wang, E. C. Cox, J. C. Sturm, P. Silberzan and R. H. Austin, *Proc. Natl. Acad. Sci. U. S. A.*, 2004, **101**, 10979–10983.

21 J. Han, S. W. Turner and H. G. Craighead, *Phys. Rev. Lett.*, 1999, **83**, 1688–1691.

22 J. A. van Kan, C. Zhang, P. P. Malar and J. R. C. van der Maarel, *Biomicrofluidics*, 2012, **6**, 036502.

23 J. A. van Kan, A. A. Bettiol and F. Watt, *Appl. Phys. Lett.*, 2003, **83**, 1629–1631.

24 J. A. van Kan, A. A. Bettiol and F. Watt, *Nano Lett.*, 2006, **6**, 579–582.

25 J. A. van Kan, P. G. Shao, Y. H. Wang and P. Malar, *Microsyst. Technol.*, 2011, **17**, 1519–1527.

26 Y. Egawa, R. Hayashida, T. Seki and J. Anzai, *Talanta*, 2008, **15**, 736–741.

27 H. S. Harned and C. L. Hildreth Jr., *J. Am. Chem. Soc.*, 1951, **73**, 650–652.

28 Y. Yuan, L. Wang and S. Amemiya, *Anal. Chem.*, 2004, **76**, 55705578.

29 F. Persson, J. Fritzsche, K. U. Mir, M. Modesti, F. Westerlund and J. O. Tegenfeldt, *Nano Lett.*, 2012, **12**, 2260–2265.

30 M. J. Allen, E. M. Bradbury and R. Balhorn, *Nucleic Acids Res.*, 1997, **25**, 2221–2226.

31 N. Makita, Y. Yoshikawa, Y. Takenaka, T. Sakaue, M. Suzuki, C. Watanabe, T. Kanai, T. Kanbe, T. Imanaka and K. Yoshikawa, *J. Phys. Chem. B*, 2011, **115**, 4453–4459.

32 N. V. Hud and I. D. Vilfan, *Annu. Rev. Biophys. Biomol. Struct.*, 2005, **34**, 295–318.